



Thermoplastic Polyurethane Blends With Thermal Energy Storage/Release Capability

Andrea Dorigato*, Daniele Rigotti and Alessandro Pegoretti

Department of Industrial Engineering and INSTM Research Unit, University of Trento, Trento, Italy

In this work innovative thermal energy storage materials were developed by encapsulating a paraffin having a melting temperature of 6°C (M6D) in a thermoplastic polyurethane (TPU), and the most important physical properties of the resulting samples were investigated from a thermo-mechanical point of view. Field emission scanning electron microscope (FESEM) micrographs demonstrated a homogeneous microcapsules distribution and good interfacial adhesion with the TPU matrix even at elevated M6D concentrations. With a capsule concentration of 60 wt% it was possible to obtain elevated melting enthalpy values (up to 95 J/g), retaining the energy storage/release properties even after 50 thermal cycles. The hardness and the dimensional stability of the TPU matrix above its glass transition temperature were strongly increased upon M6D addition, but this stiffening effect was associated to a certain embrittlement. The investigated blends could be applied for winter sport application for low temperature thermal energy storage/release materials.

Keywords: polyurethanes, blends, thermal properties, mechanical properties, energy storage

OPEN ACCESS

Edited by:

Alfonso Maffezzoli,
University of Salento, Italy

Reviewed by:

Debora Puglia,
University of Perugia, Italy
Veronique Michaud,
École Polytechnique Fédérale de
Lausanne, Switzerland

*Correspondence:

Andrea Dorigato
andrea.dorigato@unitn.it

Specialty section:

This article was submitted to
Polymeric and Composite Materials,
a section of the journal
Frontiers in Materials

Received: 14 June 2018

Accepted: 04 September 2018

Published: 26 September 2018

Citation:

Dorigato A, Rigotti D and Pegoretti A
(2018) Thermoplastic Polyurethane
Blends With Thermal Energy
Storage/Release Capability.
Front. Mater. 5:58.
doi: 10.3389/fmats.2018.00058

INTRODUCTION

Thermal energy storage (TES) materials are innovative systems able to store thermal energy through the heating of a medium, with the aim to utilize (release) the stored energy when required (on cooling). This concept was successfully applied in power generation systems (Farid et al., 2004; Demirbas, 2006; Wang et al., 2015; Zhang et al., 2016) and building constructions (Kuznik et al., 2011), applications in which about one half of the energy consumption is in the form of thermal energy, and the energy request can markedly vary in time (Kenisarin and Kenisarina, 2012; Juozapaitis et al., 2013; Robaidi, 2013). TES systems were applied in the food storage (Gin and Farid, 2010; Chen et al., 2011) and for the construction of highly efficient solar plants (Lane, 1986; Norton, 1992; Bal et al., 2010). Some innovative applications in the textiles industry of TES technology are represented by “smart” fabrics able to keep constant the temperature of the body (Shim et al., 2001; Ren and Ruckman, 2004; Shin et al., 2005; Gao et al., 2011; Sarier and Onder, 2012; Borreguero et al., 2013). In this framework, latent heat TES systems attracted the attention of the researchers, because they are characterized by an elevated energy storage density at the transition temperature of the phase change material (PCM) (Lane, 1986; Hasnain, 1998). In these materials, a solid/liquid or a solid/solid transition is generally involved and depending on their chemical nature these materials can be classified as organic, inorganic or eutectic alloys. Organic PCMs present considerable advantages (Pillai and Brinkworth, 1976; Abhat, 1983) with respect to the inorganic ones. Because of their elevated thermal storage density, wide transition temperature range interval, limited density, and low cost (Trigui et al., 2014; Sharma et al., 2015), paraffinic waxes are

the most widely used (Abhat, 1983; Himran et al., 1994; Li and Wu, 2012; Dorigato et al., 2017b). As a drawback, their limited thermal conductivity and the possible leakage above their melting point represent a serious problem to their further development (Akgün et al., 2007). In order to overcome these limitations, several shape stabilized systems with different polymer matrices, such as high-density polyethylene (HDPE) (Mu et al., 2016; Sobolciak et al., 2016), polypropylene (PP), acrylic resins, epoxy resins (Luyt and Krupa, 2009; Su et al., 2012b; Jeong et al., 2014), poly(methylmethacrylate) (PMMA), polyurethane (Pielichowska et al., 2016) block copolymer, ethylene-propylene diene monomer rubber (EPDM) (Dorigato et al., 2017b), styrene-butadiene-styrene (SBS) (Pielichowska and Pielichowski, 2014; Mu et al., 2016), polyvinylchloride (PVC) (Sari et al., 2005) were investigated. Furthermore, the PCM stabilization through the addition of nanofillers was often studied (Sari and Soyak, 2007; Pielichowska and Pielichowski, 2014; Fredi et al., 2017). Encapsulation within polymeric shells (Khadiran et al., 2015; Dorigato et al., 2017b) can be an effective solution to avoid the flow of PCM at elevated temperature (Inaba and Tu, 1997). For instance, Sari-Bey et al. investigated the potential of PCM materials constituted by a paraffinic core and a crosslinked PMMA shell (Khadiran et al., 2015). The physicochemical properties and the interface stability behavior of melamine-formaldehyde (MMF) shell microPCMs with paraffin were recently studied by Su et al. (2010, 2011). Moreover, Wang et al. investigated the correlation between the interfacial properties and mechanical performances of epoxy composites with paraffin microcapsules having a methanol-melamine-formaldehyde shell (Wang et al., 2011).

Thermoplastic polyurethanes (TPUs) are a very versatile class of elastomers, used in commodities but also for advanced applications (i.e., coatings, adhesives, biomedical devices). TPUs are random copolymers, in which the alternation of hard and soft segments determines a two-phase microstructure. Soft segments are constituted by long-chain diols, that can be extended by diisocyanate. On the other hand, while hard segments are generated by an alternation of chain extender and diisocyanate. TPUs are endowed with excellent properties, with an elasticity, tear, and abrasion resistance similar to rubber. By modifying the alternation of hard and soft segments it is possible to tailor the mechanical properties of the resulting materials. TPUs are largely applied in biomedical sector, they show interesting biodegradability properties and biostability. However, TPUs present also some limits due to poor tensile strength and low Young's modulus (Ercan et al., 2017; Fortunati et al., 2017).

Among different processing techniques suitable for TPUs, additive manufacturing technologies were recently introduced. In particular, fused filament fabrication (FFF) of TPUs gives the possibility to produce cellular structures that can be adapted for specific applications. In a paper of Bates et al. (2015), 3D printed cellular TPU structures, able to withstand repeated compressions/densification cycles without failure, were prepared. The potential of fused filament fabrication for the production of novel cellular architectures, not constrained by existing manufacturing principles, was recently demonstrated. In a work of Fei et al. (2016), selective laser sintering technique (SLS) was

adopted to investigate the energy absorption capability of TPU based lattice structures, through a systematic manufacturing, testing and modeling process. In another paper of Chen et al. (2017), polymer blends of thermoplastic polyurethane (TPU) with poly(lactic acid) (PLA) nanofilled with graphene oxide (GO) were utilized for the development of 3D printed biocompatible devices.

As regards the use of TPUs in thermal energy storage applications, most of the available scientific papers are focused on the synthesis of novel TPU based polymers, to be used as solid-solid phase change materials. In a recent paper of Cao et al. (2017), hydrogen bonding was applied to increase the crystallinity and thus the latent heat involved in the melting and crystallization processes of thermoplastic poly(ethylene glycol)-based polyurethane. The obtained melting enthalpy was around 140 J/g, which is close to the best values obtained for polyurethanes.

In another paper of Liang et al. (2015), the synthesis of a terephthalic acid bis-(2-hydroxy-1-hydroxymethyl-ethyl) ester, used to develop polyurethane based PCMs with elevated thermal energy storage/release capability, was reported. The results showed that the developed materials presented a maximum phase change enthalpy of about 150 J/g. Another work of Xi et al. (2014) was focused on thermal energy storage capability of a novel TPU, obtained by a condensation reaction of 4,4'-diphenylmethane diisocyanate, polyethylene glycol and terephthalic acid bis-(2-hydroxy-1-hydroxymethyl-ethyl) ester, manifesting solid-solid phase transitions. In this case, peak transition temperatures and latent heat values in the range of 22.4–48.4°C and 143.9–153.5 J/g were respectively obtained. The reported melting enthalpy values are lower or comparable with those that could be obtained with a paraffin microencapsulated system.

On the other hand, only few papers dealing with the use of paraffin with melting temperatures lower than ambient temperature can be found in the open scientific literature (Bo et al., 1999; Pielichowska and Pielichowski, 2014; Dorigato et al., 2017a). In fact, the dispersion of a liquid wax in a viscous polymer poses some practical difficulties due to the remarkably different rheological behavior of the two phases. Nevertheless, these systems could offer challenging opportunities for low temperature applications such as those regarding winter sport products. Based on these considerations, the aim of the present work is the development and characterization of polymer blends in which microcapsules containing a low melting (6°C) paraffin were dispersed in a commercial TPU matrix by melt compounding. Thus, the results of this paper represent a complementary part of a wider research activity aimed at developing 3D printed structures with thermal energy storage/release capability based on TPU/paraffin blends, to be utilized in winter sport applications (i.e., gloves or insoles; Rigotti et al., 2018).

EXPERIMENTAL

Materials

TPU chips of Desmopan® 6064A (density 1.09 g/cm³, melting temperature range 200–220°C) were provided by Covestro Italia

(Milan, Italy). Microtek MPCM6D microcapsules (designated as M6D in this paper) were supplied by Microtek Laboratories Inc. [Dayton (OH, USA)]. In this PCM, a paraffin wax is contained in a melamine formaldehyde polymeric shell. The microcapsules have an average size of 17–20 μm and a density of 0.9 g/cm^3 . They are constituted by 10–15 wt% of polymer shell and by 85–90 wt% of paraffin. According to the producer's data sheet, the melting enthalpy is 157–167 J/g and the melting temperature is about 6°C.

Preparation of the Samples

TPU granules and M6D microcapsules were melt compounded with various amounts of M6D microcapsules (ranging from 30 to 60 wt%). The blends were prepared in a Thermo Haake Rheomix 600 internal mixer, equipped with counter-rotating rotors, operating at 60 rpm for 5 min at 200°C. The resulting materials were then hot pressed in a Carver laboratory press at 180°C for 15 min under a pressure of 1.1 MPa applied on square plates of 300 \times 300 mm^2 . In this way, plaques of neat TPU and blends at various PCM concentrations were obtained. In this paper, the neat matrix was simply designated as TPU, while the blends were denoted reporting the matrix and the microcapsules concentration. As an example, TPU_50M6D sample indicates a TPU blend containing 50 wt% of M6D microcapsules. In **Table 1** the list of the prepared samples with the weight and volume fraction of paraffin within the blends is reported.

Experimental Techniques

Microstructural and Thermal Properties

The microstructure of the prepared blends was investigated through a Zeiss Supra 40 field emission scanning electron microscope (FESEM). Before the observation, samples were cryofractured in liquid nitrogen and the surface coated with an ultrathin coating of electrically conductive Pt/Pd material.

Differential scanning calorimetry (DSC) tests were performed with a Mettler DSC30 under a nitrogen flux of 150 ml/min, at a heating rate of 10°C/min, starting from –100°C up to 220°C. In this way, melting/crystallization temperatures (T_m , T_c), melting/crystallization enthalpies (ΔH_m , ΔH_c) of the microcapsules and the glass transition temperature (T_g) of the TPU matrix were determined. Moreover, relative melting ($\Delta H_{m,rel}$) and crystallization ($\Delta H_{c,rel}$) enthalpy values were computed as the ratio between the ΔH_m and ΔH_c and the melting/crystallization enthalpies of the M6D capsules, considering the microcapsule concentration in the composites. In order to determine the retention of the thermal energy storage properties of the prepared blends, repeated DSC tests

were performed on the TPU_50M6D samples. In particular, fifty heating/cooling cycles in the temperature interval between –35 and 45°C were performed at a heating rate of 10°C/min and ΔH_m and ΔH_c values were measured at each cycle. Only one specimen was tested for each composition.

Thermogravimetric analysis (TGA) was performed through a TA Instruments TGAQ500 machine in nitrogen atmosphere, testing samples between 30 and 700°C, at a heating rate of 10°C/min. In this way, the temperatures associated to a mass loss of the 2% ($T_{2\%}$), of the 5% ($T_{5\%}$), of the 10% ($T_{10\%}$) and the decomposition temperature (T_d), taken as the temperature corresponding to the maximum mass loss rate, were defined. Only one specimen was tested for each composition.

Thermo-Mechanical Properties

Dynamical mechanical thermal analysis (DMTA) was carried out through a TA Instruments DMA Q800 analyzer in tensile mode, testing rectangular specimens with a length of 30 mm, a width of 5 mm wide and a thickness of 1 mm. The investigated temperature range was between –60 and 100°C scanned at a heating rate equal to 3°C/min, the testing frequency was 1 Hz, the strain amplitude was 0.05 mm/mm. In this way, the trends of the storage (E') and loss (E'') moduli and of the loss tangent ($\tan\delta$) as a function of the temperature were highlighted. Moreover, the glass transition temperature of the TPU (T_g) was determined. Only one specimen was tested for each composition.

Uniaxial quasi-static tensile tests were performed at a cross-head speed of 100 mm/min by using an Instron model 5969 machine, equipped with a load cell of 50 kN. A resistance extensometer Instron model 2630, having a gauge length of 25 mm, was utilized. Five ISO 527 1BA dumbbell specimens were tested for each sample. It was therefore possible to determine the chord modulus at a deformation of the 10% ($E_{10\%}$), the stress (σ_b) and the strain at break (ϵ_b). At least five specimens were tested for each formulation.

Shore A hardness tests were performed at room temperature with a Hildebrand Durometer OS-2. According to the DIN 53505 standard, Shore A values were recorded after that the load was applied for 3 s. At least five specimens were tested for each composition.

Creep tests were carried out through a TA Instruments DMA Q800 machine. Rectangular specimens (length = 30 mm, width = 5 mm, thickness = 1 mm) were tested at 30°C, under an applied stress of 0.25 MPa for 3,600 s. In this way, the trend of the creep compliance, obtained as the ratio between the creep deformation and the constant stress, as a function of the testing time was determined. Only one specimen was tested for each composition.

TABLE 1 | List of the prepared samples.

| Sample | M6D content [wt%] | M6D content [vol%] |
|-----------|-------------------|--------------------|
| TPU | – | – |
| TPU_30M6D | 30.0 | 34.2 |
| TPU_40M6D | 40.0 | 44.7 |
| TPU_50M6D | 50.0 | 54.8 |
| TPU_60M6D | 60.0 | 64.5 |

RESULTS AND DISCUSSION

Microstructural and Thermal Properties

Considering that the thermo-mechanical properties of polymeric materials are strictly related to their morphological behavior, FESEM analysis was carried out on the prepared samples. In **Figures 1A–D** FESEM micrographs of the neat TPU and of the relative blends are reported. Some porosity can be detected in

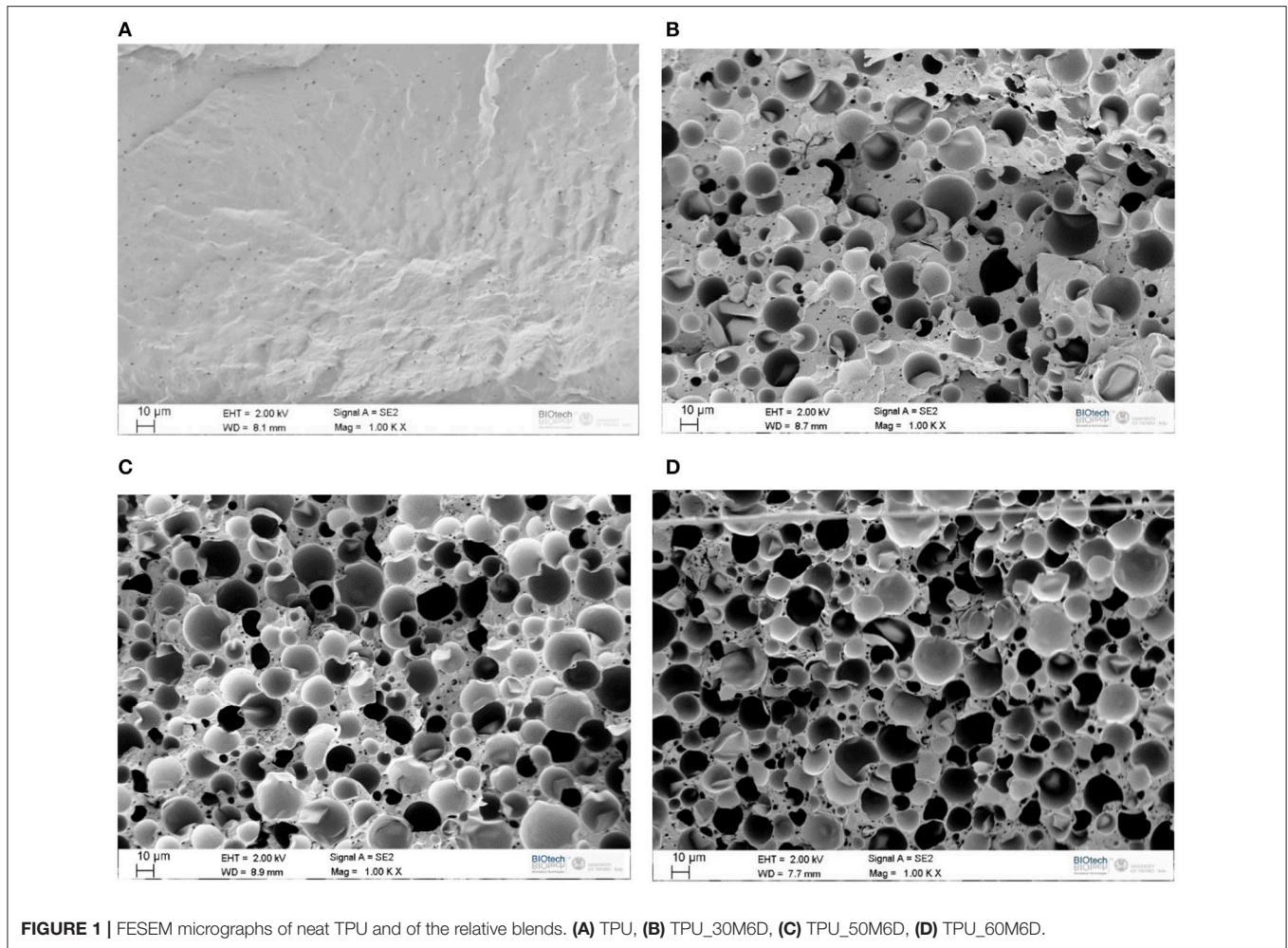


FIGURE 1 | FESEM micrographs of neat TPU and of the relative blends. **(A)** TPU, **(B)** TPU_30M6D, **(C)** TPU_50M6D, **(D)** TPU_60M6D.

the TPU matrix in form of very small rounded cavities with mean diameter ranging from 1 to 5 μm (see **Figure 1A**). In the micrographs of the blends prepared at different concentrations it can be noticed the presence of the capsules with diameter up to 20 μm . From these images, a good adhesion between TPU and the melamine-formaldehyde resin shell of the microcapsules can be detected. The elevated adhesion level with the TPU matrix is probably the reason why some microcapsules were broken during the cryofracturing operations (see **Figure 1B**). Furthermore, no microcapsules agglomeration can be seen in the composites, and the uniform distribution of M6D capsules determines a morphological continuity of the matrix even at elevated M6D contents. This aspect can strongly influence the mechanical properties and the thermal conductivity of the resulting samples. The micrometric porosity detected in the neat TPU sample is also present in the blends, regardless the M6D amount.

Considering that the thermal energy storage properties of the prepared materials is a key feature for their future application, DSC tests were carried out. In **Figures 2A,B** the heating and cooling DSC thermograms of neat TPU, neat M6D capsules and their blends are respectively reported, while the main thermal parameters are summarized in **Table 2**. In **Figure 2A** it can be

seen that neat TPU presents a perfectly flat thermogram, without crystallization and/or melting signals from -100 to 220°C , and only an inflection point associated to the glass transition temperature (T_g) can be detected at -48°C . The melting peak of the M6D capsules is located at 5°C in the heating stage, while the crystallization temperature is at -9°C in the cooling stage. The specific heat of fusion is 157.4 J/g, while the heat of crystallization is 163.5 J/g, these values are very close to the data provided by the producer. Another small peak can be seen during the heating stage at around 34°C , with a specific enthalpy of 5 J/g. This is probably due to the presence of some paraffin fractions at higher molecular weight. Considering the relative low intensity of this peak and the fact that it is in a temperature range that is not relevant for the intended application of this materials, this signal was not taken into account during the calculations.

It is interesting to note how the melting enthalpy values during the first heating stage ($\Delta H_{m,1}$) are proportional to the M6D content. A melting enthalpy value as high as 95.1 J/g was detected for the TPU_60M6D sample. Moreover, considering that the reported $\Delta H_{m,rel}$ values are very close to 100%, it can be concluded that the selected compounding process is able to preserve the microcapsules integrity thus preventing

paraffin leakage. The position of the melting and crystallization temperature does not seem to be substantially affected by the capsules concentration within the TPU matrix. It is also interesting to note that the $\Delta H_{c,rel}$ and $\Delta H_{m2,rel}$ values are slightly lower than the corresponding $\Delta H_{m1,rel}$ values, meaning

that after the first heating/cooling cycle a slight reduction of the thermal energy storage/release capabilities is observed in the blends, probably due to some paraffin leakage phenomena. However, the thermal effectiveness of the prepared materials is confirmed, being the $\Delta H_{c,rel}$ and $\Delta H_{m2,rel}$ values higher than 80% for all the tested compositions.

According to the information reported in their datasheet, M6D microcapsules should support repeated thermal cycles. However, their effectiveness should be tested after compounding in the TPU matrix. Therefore, repeated DSC measurements were carried out, to assess if the thermal properties of the prepared blends are maintained even after repeated thermal cycles. It can be also noticed that both T_{m1} and T_{m2} of the microcapsules in the blends are slightly increased when they are incorporated in the TPU matrix (by about 2–3°C), while the T_c are progressively decreased with the M6D amount. This is probably only a thermal effect due to the heat conduction within the TPU matrix, and the effective temperature within the capsules is lower than those imposed by the thermal ramp during the DSC tests.

In **Figure 3** the fusion and crystallization heat values are reported as a function of the number of DSC cycles for the TPU_50M6D sample. It results that ΔH_m values oscillates

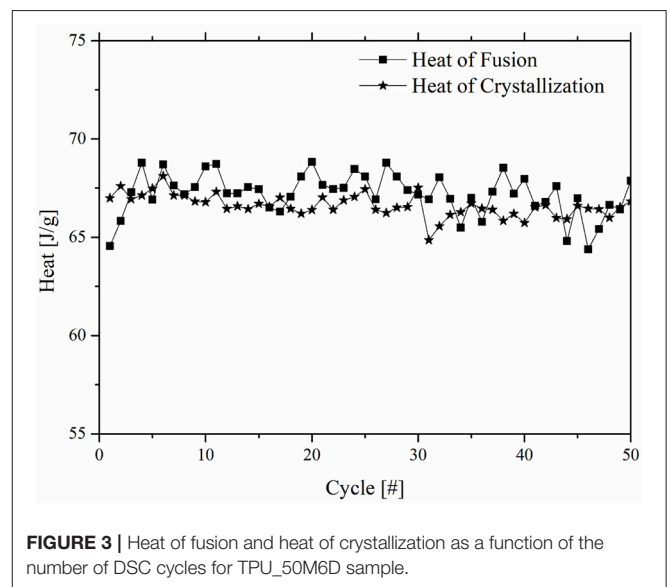
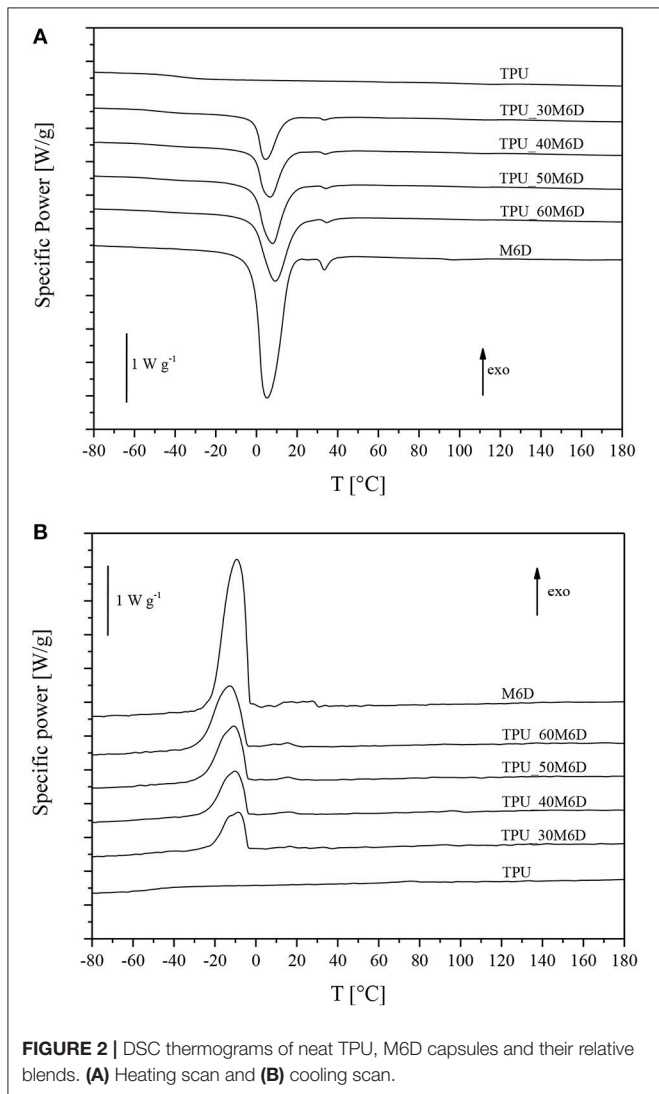


TABLE 2 | Results of DSC tests on neat TPU and its relative polymer blends.

| Samples | T_g [°C] | $T_{m,1}$ [°C] | $\Delta H_{m,1}$ [J/g] | $\Delta H_{m1,rel}$ [%] | T_c [°C] | ΔH_c [J/g] | $\Delta H_{c,rel}$ [%] | $T_{m,2}$ [°C] | $\Delta H_{m,2}$ [J/g] | $\Delta H_{m2,rel}$ [%] |
|-----------|------------|----------------|------------------------|-------------------------|------------|--------------------|------------------------|----------------|------------------------|-------------------------|
| TPU | -48.0 | - | - | - | - | - | - | - | - | - |
| TPU_30M6D | - | 6.6 | 45.6 | 95.9 | -8.6 | 42.1 | 88.5 | 4.3 | 39.2 | 83.3 |
| TPU_40M6D | - | 8.0 | 56.1 | 88.3 | -10.1 | 52.6 | 83.1 | 6.8 | 50.3 | 80.2 |
| TPU_50M6D | - | 8.8 | 74.9 | 94.6 | -10.7 | 64.7 | 81.7 | 8.0 | 69.1 | 88.0 |
| TPU_60M6D | - | 9.5 | 92.1 | 96.7 | -12.9 | 79.6 | 83.7 | 9.2 | 80.1 | 84.8 |
| M6D | - | 5.0 | 158.5 | 100 | -9.4 | 158.4 | 100 | 5.1 | 157.1 | 100 |

T_g , glass transition temperature of TPU; $T_{m,1}$, melting temperature (first heating stage); $\Delta H_{m,1}$, experimental melting enthalpy (first heating stage); $\Delta H_{m1,rel}$, normalized melting enthalpy (first heating stage); T_c , crystallization temperature (cooling stage); ΔH_c , experimental crystallization enthalpy; $\Delta H_{c,rel}$, normalized crystallization enthalpy; $T_{m,2}$, melting temperature (second heating stage); $\Delta H_{m,2}$, experimental melting enthalpy (second heating stage); $\Delta H_{m2,rel}$, normalized melting enthalpy (second heating stage).

between 65 and 69 J/g, while ΔH_c values varies between 66 and 68 J/g, without any clear trend with the number of DSC cycles. From this result it is possible to establish that the prepared materials can withstand repeated thermal cycles (at least 50), without losing their thermal energy storage/release capability.

Thermogravimetric analysis was carried out to assess the thermal degradation resistance of the prepared blends. In **Figure 4A**, thermogravimetric curves of neat TPU and its relative blends are reported, while in **Figure 4B** derivative TGA curves are represented. In **Table 3** the most important results are summarized. For all the prepared samples, the main degradation step starts at temperatures higher than 300°C, but there are other two degradation steps to be considered. Above 100°C there is an initial degradation step for the blends, and the magnitude of this mass loss (even if not so pronounced) is proportional to the M6D content. This is the reason why $T_{2\%}$, $T_{5\%}$, and $T_{10\%}$ values of the blends are lower than those reported for the neat TPU (see **Table 3**). It can be supposed that some microcapsules break during the melt compounding/hot pressing processes,

and the leaked paraffin could then easily evaporate at relatively low temperature. This hypothesis is supported by the slight lowering of the relative melting/crystallization enthalpy values detected in DSC tests during the cooling/second heating scan. Another interesting aspect is that, differently from the neat TPU sample, in the blends there is some residual ash (2–4%), that can be attributed to the material associated to microcapsules shell (i.e., melamine-formaldehyde resin). Interestingly, M6D addition promotes an increase of T_d values (even by 42°C with a M6D concentration of 40%), and from **Figure 4B** two distinct degradation steps can be detected for the blends in the temperature interval between 300 and 500°C. This behavior is probably due to the presence of a crosslinked organic shell in the blends, with a superior thermal resistance as compared to the TPU matrix that partially protects the paraffin from thermal degradation.

Thermo-Mechanical Properties

To assess the potentialities of these materials in improving thermal management for winter sports application, it is important to evaluate the effect of M6D addition on the mechanical behavior of the resulting blends and how the mechanical response change with temperature. In **Figures 5A–C**, the results of DMTA tests on neat TPU and relative blends are reported in terms of their storage and loss moduli and loss tangent, while in **Table 4** the glass transition temperatures (T_g) values are reported. A very interesting aspect is that at temperatures lower than -30°C there is a decreasing trend of storage modulus with the microcapsules content, while this trend is the opposite at higher temperatures. This behavior indicates that below the glass transition temperature of the TPU matrix the stiffness of the microcapsules is lower than that of the TPU, while the opposite happens above T_g . Furthermore, from the analysis of E'' and $\tan\delta$ plots (**Figures 5B,C**) it is possible to note that as the content of M6D decreases the peaks become more intense and narrower. According to the indications reported in the open scientific literature (Menard, 2008), T_g values reported in **Table 4** have been determined in three different ways, i.e., considering the position of the E' inflection point (T_{g1}), the temperature associated to the E'' peak (T_{g2}) and to the $\tan\delta$ peak (T_{g3}). In the case of amorphous polymers, the value of T_{g3} is much

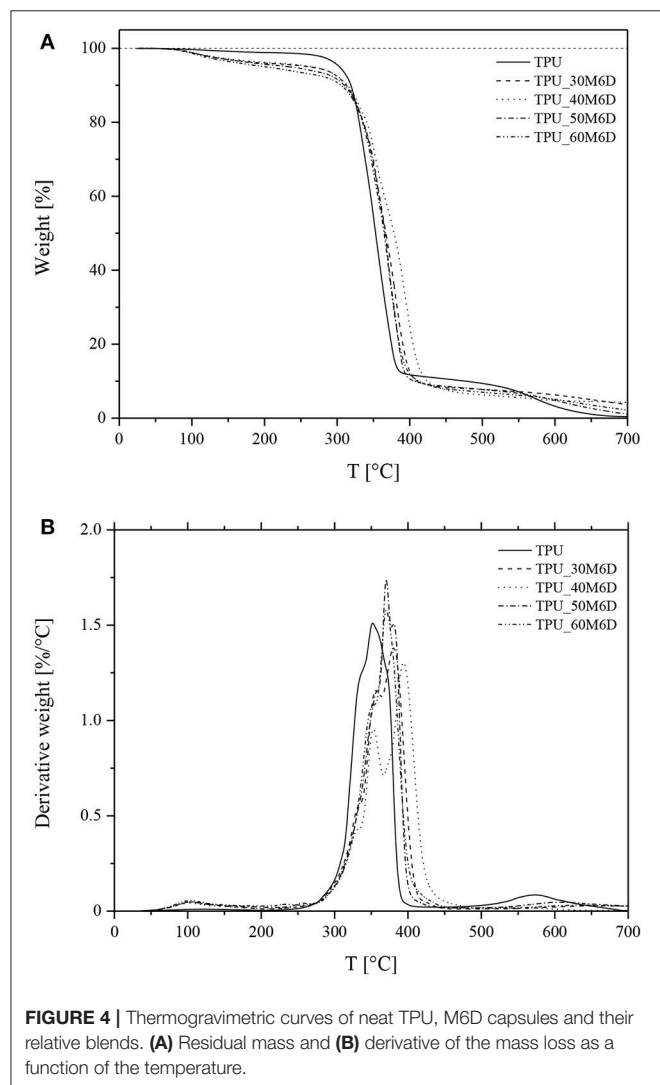
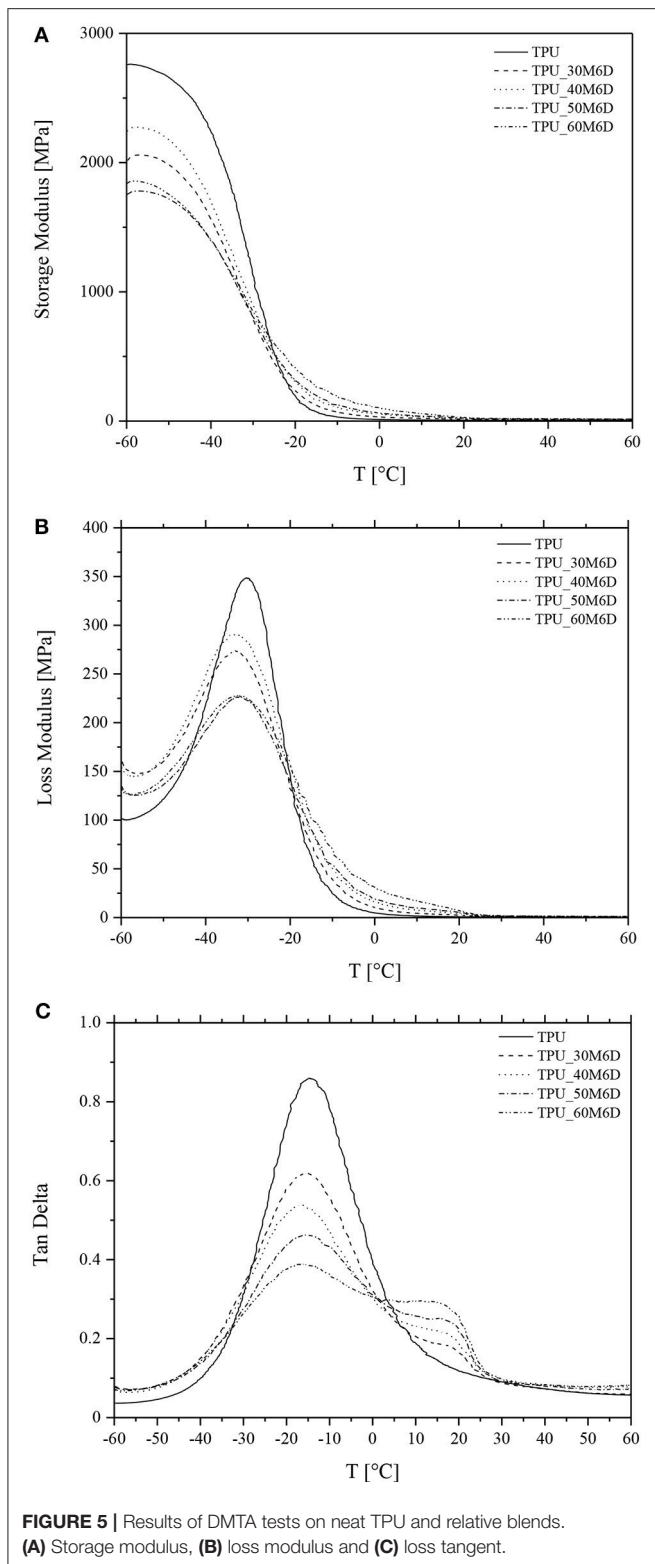


TABLE 3 | Results of thermogravimetric test on neat TPU and relative blends.

| Samples | $T_{2\%}$ [°C] | $T_{5\%}$ [°C] | $T_{10\%}$ [°C] | T_d [°C] |
|-----------|----------------|----------------|-----------------|------------|
| TPU | 274 | 304 | 319 | 351 |
| TPU_30M6D | 119 | 261 | 313 | 380 |
| TPU_40M6D | 121 | 266 | 314 | 393 |
| TPU_50M6D | 119 | 234 | 310 | 370 |
| TPU_60M6D | 112 | 202 | 305 | 370 |

$T_{2\%}$, temperature associated to a mass loss of 2%; $T_{5\%}$, temperature associated to a mass loss of 5%; $T_{10\%}$, temperature associated to a mass loss of 10%; T_d , degradation temperature (temperature associated to the maximum mass loss rate).



higher than T_{g1} and T_{g2} , because it implies a different mode of molecular motion. It was demonstrated in literature that T_{g1} and T_{g2} signals are due to the local segmental motion of the macromolecules, while T_{g3} can be attributed to the transition

TABLE 4 | Glass transition temperatures (T_g) values from DMTA tests on neat TPU and relative blends.

| Samples | T_{g1} [°C] | T_{g2} [°C] | T_{g3} [°C] | Shore A hardness |
|-----------|---------------|---------------|---------------|------------------|
| TPU | -43.4 | -30.2 | -14.4 | 66 ± 1 |
| TPU_30M6D | -46.6 | -32.6 | -15.3 | 76 ± 1 |
| TPU_40M6D | -47.2 | -33.0 | -16.6 | 76 ± 1 |
| TPU_50M6D | -45.5 | -32.0 | -15.2 | 79 ± 1 |
| TPU_60M6D | -47.0 | -32.1 | -16.2 | 81 ± 1 |

Results of Shore A hardness tests on neat TPU and of the relative blends. T_{g1} , taken as the temperature associated to the inflection point in E' curves; T_{g2} , taken as the temperature associated to the E' peak; T_{g3} , taken as the temperature associated to the $\tan\delta$ peak.

of entropic Rouse modes, thus cannot be properly considered as the glass transition temperature of the material (Lei et al., 2014). However, from **Table 4** it can be concluded that the glass transition temperature of the materials slightly decreases with the M6D content (by about 3–4°C). This drop, even if not so pronounced, could be attributed to the plasticizing effect played by the wax leaked from the capsules broken under the processing steps. However, further investigation should be performed to reach a better comprehension of this aspect. Another feature that can be observed in $\tan\delta$ curves is the presence of a shoulder at about 10–15°C only in samples with microcapsules, especially at elevated M6D concentrations. Through a comparison with DSC tests it can be concluded that this signal can be associated to the melting of paraffin inside the microcapsules. The viscoelastic behavior of the material near ambient temperature could be strongly determined by the paraffin melting of the paraffin inside the microcapsules.

It is therefore important to quantify the effect of microcapsules on the ultimate properties of the investigated materials. Representative stress-strain curves in quasi-static tensile conditions of neat TPU and relative blends are represented in **Figure 6A**. The most important mechanical parameters are summarized in **Figure 6B**. It must be pointed out that the neat TPU sample did not reach the failure and the tests was stopped at a strain $\epsilon = 3$ mm/mm, in order to preserve the integrity of the extensometer. According to DMTA results, it is possible to notice that a stiffness increase is induced by M6D capsules (from 5 up to 15 MPa with a M6D amount of 60%). After the elastic region, the blends manifest a progressive flattening of the stress-strain curves, probably due to the debonding between the TPU matrix and the capsules at high deformation, followed by the failure of the samples at relatively low strain levels. From the data reported in **Table 4**, it is possible to conclude that the addition of M6D capsules promotes an evident stiffening, accompanied to a certain embrittlement. In fact, stress at break is negatively affected by M6D addition, and this behavior is even more pronounced if strain at break values are considered. The stiffening effect played by the microcapsules is confirmed by Shore A hardness measurements. In fact, as reported in **Table 4**, Shore A hardness increases from 66 for the neat TPU up to 81 for the TPU_60M6D sample.

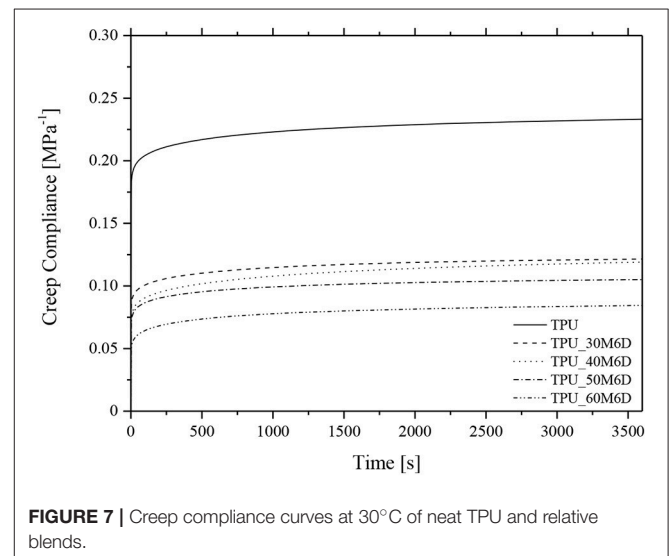
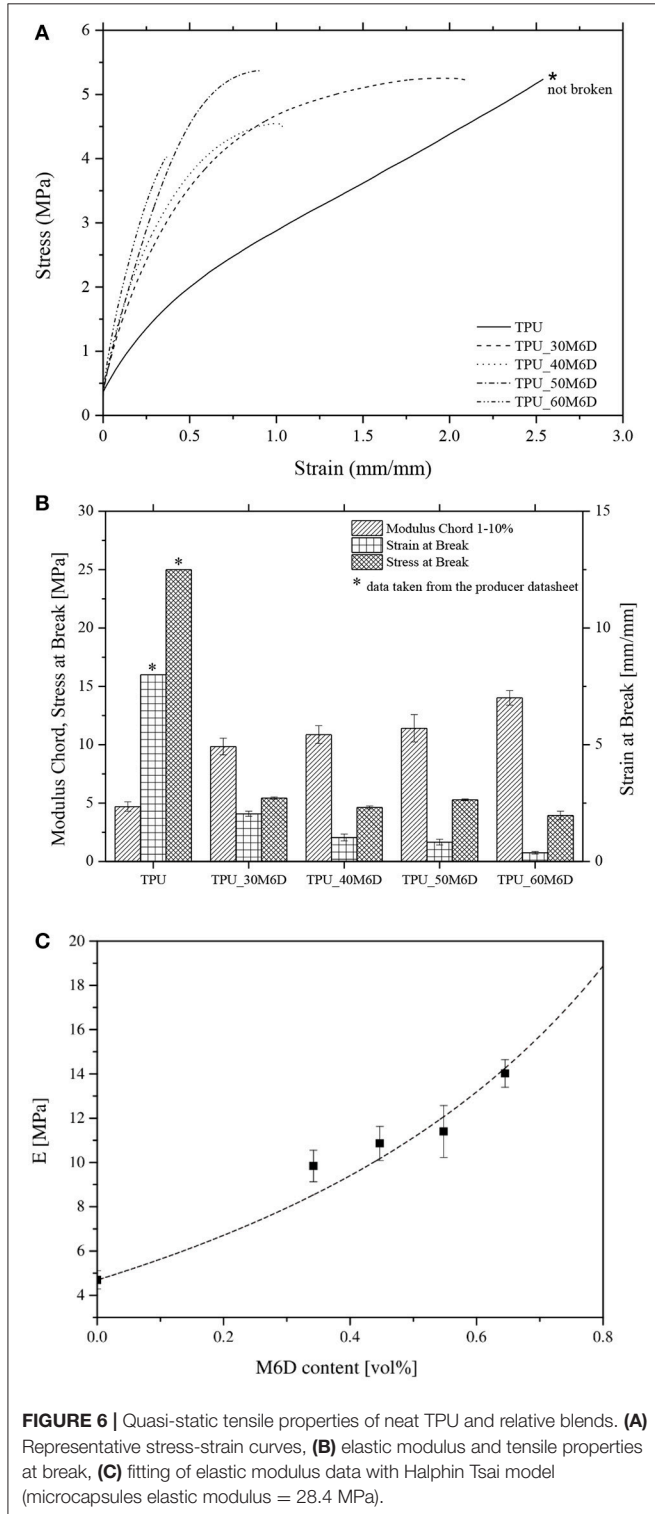
It could be also interesting to interpret elastic modulus results by considering theoretical models traditionally used for particulate composites. The prediction of modulus of the prepared materials was modeled by the Halpin-Tsai micromechanical model, which is a well-known theory to predict

stiffness of composites as a function of filler loading and aspect ratio (Halpin, 1969). The predicted modulus of a particulate filled polymer (E_c) is given by the expression reported in Equations (1) and (2):

$$E_c = E_m \frac{1 + 2\eta V_f}{1 - \eta V_f} \tag{1}$$

$$\eta = \frac{\frac{E_f}{E_m} - 1}{\frac{E_f}{E_m} + 2} \tag{2}$$

where E_f and E_m are, respectively, the elastic modulus of the filler and of the matrix (i.e., 4.69 MPa). In **Figure 6C** elastic modulus data of the prepared samples are fitted with Halpin Tsai model. It is clear that the results strongly depend on the elastic modulus of the microcapsules. Through the least square minimization procedure, it was possible to determine the best fitting curve by imposing a microcapsule elastic modulus of 28.4 MPa. From **Figure 6C** it is evident that in these conditions it is possible to satisfactorily predict the stiffness of the prepared materials. In literature little data are available on the stiffness of microencapsulated system, and the greatest part of the paper tried to determine the micromechanical behavior of the capsules through nanoindentation tests. In a recent study performed by Su et al. nanoindentation was successfully applied to measure the micromechanical properties of microcapsules containing paraffin (Su et al., 2012a). In that paper, a series of melamine formaldehyde shell microcapsules were prepared with various size and thickness by controlling the core material stirring rates, producing capsules having micrometric dimensions and with core/shell ratios ranging from 1/1 to 1/3. It was found that elastic modulus of the produced microcapsules was in the range 1.5–2.7 GPa. By using these values in the present fitting, an excessive overestimation of the theoretical values would result. In the present case, the situation is very different and a lower E_f value must be adopted (i.e., 28.4 MPa), probably



because the core/shell ratio is rather high (85/15), and the paraffin at ambient temperature is in the molten state. In order to validate this theoretical prediction, nanoindentation tests will be performed in the future on these PCM systems.

Considering the intended application of the prepared blends, it could be interesting also to further study the viscoelastic response of these materials under a constant applied load. For this reason, creep tests were performed. Creep compliance curves of neat TPU and of the relative blends at 30°C are reported in **Figure 7**. It is possible to note that at 30°C no tertiary creep is detectable, in fact all the samples reach the characteristic plateau of the secondary creep even after 3,600 s. In accordance with quasi-static and DMTA tests, by increasing M6D content the creep compliance strongly decreases, confirming thus the stabilizing effect played by paraffin microcapsules on the TPU matrix.

CONCLUSIONS

Innovative TPU/encapsulated paraffin blends to be applied as thermal energy storage/release materials for winter sports applications were successfully developed. FESEM analysis

revealed a homogeneous distribution of the microcapsules and a good interfacial adhesion with the TPU matrix even at elevated M6D loadings. DSC test demonstrated how it was possible to prepare blends with melting enthalpy values up to 95 J/g with a M6D concentration of 60% and able to retain most of their pristine energy storage capability even after repeated thermal cycles. The hardness and the dimensional stability of the resulting blends above the T_g of the TPU matrix were significantly improved upon M6D addition, even if the observed stiffening effect was accompanied by a certain embrittlement of the samples.

AUTHOR CONTRIBUTIONS

AD and DR performed part of the experimental work and contributed to the preparation of the manuscript. AP contributed to the preparation of the manuscript.

ACKNOWLEDGMENTS

Mr. Giuliano Barp is gratefully acknowledged for his support to the experimental work. Dr. Luca Alborghetti of Covestro Italia is kindly acknowledged for the provision of TPU.

REFERENCES

- Abhat, A. (1983). Low temperature latent heat thermal energy storage: heat storage materials. *Solar Energy* 30, 313–332. doi: 10.1016/0038-092X(83)90186-X
- Akgün, M., Aydin, O., and Kaygusuz, K. (2007). Experimental study on melting/solidification characteristics of a paraffin as PCM. *Energy Convers. Manag.* 48, 669–678. doi: 10.1016/j.enconman.2006.05.014
- Bal, L. M., Satya, S., and Naik, S. N. (2010). Solar dryer with thermal energy storage systems for drying agricultural food products: a review. *Renew. Sustain. Energy Rev.* 14, 2298–2314. doi: 10.1016/j.rser.2010.04.014
- Bates, S. R. G., Farrow, I. R., and Trask, R. S. (2015). 3D printed polyurethane honeycombs for repeated tailored energy absorption. *Mat. Design* 112, 172–183. doi: 10.1016/j.matdes.2016.08.062
- Bo, H., Gustafsson, E. M., and Setterwall, F. (1999). Tetradecane and hexadecane binary mixtures as phase change materials (PCMs) for cool storage in district cooling systems. *Energy* 24, 1015–1028. doi: 10.1016/S0360-5442(99)00055-9
- Borreguero, A. M., Talavera, B., Rodriguez, J. F., Valverde, J. L., Gonzalez, J. L., and Carmona, M. (2013). Enhancing the thermal comfort of fabrics for the footwear industry. *Text. Res. J.* 83, 1754–1763. doi: 10.1177/0040517513481872
- Cao, H., Qi, F., Liu, R., Wang, F., Zhang, C., Zhang, X., et al. (2017). The influence of hydrogen bonding on N-methyl-diethanolamine-extended polyurethane solid-solid phase change materials for energy storage. *RSC Adv.* 7, 11244–11252. doi: 10.1039/C7RA00405B
- Chen, C.-R., Chou, H.-M., and Lan, N. V. (2011). “Effective heat utilization for energy saving in food and beverage thermal isolated containers,” in *International Conference on Consumer Electronics, Communications and Networks (CECNet)* (Xianning), 4945–4948.
- Chen, Q., Mangadiao, J. D., Wallat, J., De Leon, A., Pokorski, J. K., and Advincula, R. C. (2017). 3D printing biocompatible Polyurethane/Poly(lactic acid)/Graphene Oxide nanocomposites: anisotropic properties. *ACS Appl. Mat. Interf.* 9, 4015–4023. doi: 10.1021/acsami.6b11793
- Demirbas, M. F. (2006). Thermal energy storage and phase change materials: an overview. *Energy Sour. B Econ. Plan. Policy* 1, 85–95. doi: 10.1080/009083190881481
- Dorigato, A., Canclini, P., Unterberger, S. H., and Pegoretti, A. (2017a). Phase changing nanocomposites for low temperature thermal energy storage and release. *Expr. Polymer Lett.* 11, 738–752. doi: 10.3144/expresspolymlett.2017.71
- Dorigato, A., Ciampolillo, M. V., Cataldi, A., Bersani, M., and Pegoretti, A. (2017b). Polyethylene wax/EPDM blends as shape-stabilized phase change materials for thermal energy storage. *Rubber Chem. Technol.* 90, 575–584. doi: 10.5254/rct.82.83719
- Ercan, N., Durmus, A., and Kasgoz, A. (2017). Comparing of melt blending and solution mixing methods on the physical properties of thermoplastic polyurethane/organoclay nanocomposite films. *J. Thermoplast. Compos. Mat.* 30, 950–970. doi: 10.1177/0892705715614068
- Farid, M. M., Khudhair, A. M., Razack, S. A. K., and Al-Hallaj, S. (2004). A review on phase change energy storage: materials and applications. *Energy Convers. Manag.* 45, 1597–1615. doi: 10.1016/j.enconman.2003.09.015
- Fei, S., Shangqin, Y., and Yanchunni, G. (2016). Energy absorption of thermoplastic polyurethane lattice structures via 3D printing: modeling and prediction. *Int. J. Appl. Mech.* 8:1640006 doi: 10.1142/S1758825116400068
- Fortunati, E., Luzi, F., Janke, A., Haußler, L., Pionteck, J., Kenny, J. M., et al. (2017). Reinforcement effect of cellulose nanocrystals in thermoplastic polyurethane matrices characterized by different soft/hard segment ratio. *Polymer Eng. Sci.* 57, 521–530. doi: 10.1002/pen.24532
- Fredi, G., Dorigato, A., Fambri, L., and Pegoretti, A. (2017). Wax confinement with carbon nanotubes for phase changing epoxy blends. *Polymers* 9, 405–420. doi: 10.3390/polym9090405
- Gao, C., Kuklane, K., and Holmér, I. (2011). Cooling vests with phase change materials: the effects of melting temperature on heat strain alleviation in an extremely hot environment. *Eur. J. Appl. Physiol.* 111, 1207–1216. doi: 10.1007/s00421-010-1748-4
- Gin, B., and Farid, M. M. (2010). The use of PCM panels to improve storage condition of frozen food. *J. Food Eng.* 100, 372–376. doi: 10.1016/j.jfoodeng.2010.04.016
- Halpin, J. C. (1969). Stiffness and expansion estimates for oriented short fiber composites. *J. Compos. Mater.* 3, 720–724. doi: 10.1177/002199836900300416
- Hasnain, S. M. (1998). Review on sustainable thermal energy storage technologies, Part I: heat storage materials and techniques. *Energy Convers. Manag.* 39, 1127–1138. doi: 10.1016/S0196-8904(98)00025-9
- Himran, S., Suwono, A., and Mansoori, G. A. (1994). Characterization of alkanes and paraffin waxes for application as phase change energy storage medium. *Energy Sour.* 16, 117–128. doi: 10.1080/00908319408909065

- Inaba, H., and Tu, P. (1997). Evaluation of thermophysical characteristics on shape-stabilized paraffin as a solid-liquid phase change material. *Heat Mass Transf.* 32, 307–312. doi: 10.1007/s002310050126
- Jeong, S. G., Cha, J., Kim, S., Seo, J., Lee, J. H., and Kim, S. (2014). Preparation of thermal-enhanced epoxy resin adhesive with organic PCM for applying wood flooring. *J. Therm. Anal. Calorim.* 117, 1027–1034. doi: 10.1007/s10973-014-3862-8
- Juozapaitis, A., Vainiunas, P., Zavadskas, E. K., Ostry, M., and Charvat, P. (2013). Modern building materials, structures and techniques materials for advanced heat storage in buildings. *Proc. Eng.* 57, 837–843. doi: 10.1016/j.proeng.2013.04.106
- Kenisarin, M. M., and Kenisarina, K. M. (2012). Form-stable phase change materials for thermal energy storage. *Renew. Sustain. Energy Rev.* 16, 1999–2040. doi: 10.1016/j.rser.2012.01.015
- Khadiran, T., Hussein, M. Z., Zainal, Z., and Rusli, R. (2015). Encapsulation techniques for organic phase change materials as thermal energy storage medium: a review. *Solar Energy Mat. Solar Cells* 143, 78–98. doi: 10.1016/j.solmat.2015.06.039
- Kuznik, F., David, D., Johannes, K., and Roux, J. J. (2011). A review on phase change materials integrated in building walls. *Renew. Sus. Energy Rev.* 15, 379–391. doi: 10.1016/j.rser.2010.08.019
- Lane, G. (1986). *Solar Heat Storage: Latent Heat Materials, Vol. II*. Florida, FL: CRC Press; Technology,
- Lei, Z., Xing, W., Wu, J., Huang, G., Wang, X., and Zhao, L. (2014). The proper glass transition temperature of amorphous polymers on dynamic mechanical spectra. *J. Therm. Anal. Calorim.* 116, 447–453. doi: 10.1007/s10973-013-3526-0
- Li, M., and Wu, Z. (2012). A review of intercalation composite phase change material: preparation, structure and properties. *Renew. Sus. Energy Rev.* 16, 2094–2101. doi: 10.1016/j.rser.2012.01.016
- Liang, P., Xi, P., Cheng, B. W., Wang, X. Q., and Zhang, Y. Q. (2015). Synthesis and performance of thermoplastic polyurethane-based solid-solid phase-change materials for energy storage. *Sci. Adv. Mat.* 7, 2420–2426. doi: 10.1166/sam.2015.2421
- Luyt, A. S., and Krupa, I. (2009). Phase change materials formed by UV curable epoxy matrix and Fischer-Tropsch paraffin wax. *Energy Convers. Manag.* 50, 57–61. doi: 10.1016/j.enconman.2008.08.026
- Menard, H. P. (2008). *Dynamic Mechanical Analysis: A Practical Introduction, 2nd Edn*. Boca Raton, FL: CRC Press.
- Mu, M. L., Basheer, P. A. M., Sha, W., Bai, Y., and McNally, T. (2016). Shape stabilised phase change materials based on a high melt viscosity HDPE and paraffin waxes. *Appl. Energy* 162, 68–82. doi: 10.1016/j.apenergy.2015.10.030
- Norton, B. (1992). *Solar Energy Thermal Technology*. Heidelberg: Springer-Verlag. doi: 10.1007/978-1-4471-1742-1
- Pielichowska, K., Bieda, J., and Szatkowski, P. (2016). Polyurethane/graphite nanoplatelet composites for thermal energy storage. *Renew. Energy* 91, 456–465. doi: 10.1016/j.renene.2016.01.076
- Pielichowska, K., and Pielichowski, K. (2014). Phase change materials for thermal energy storage. *Prog. Mat. Sci.* 65, 67–123. doi: 10.1016/j.pmatsci.2014.03.005
- Pillai, K. K., and Brinkworth, B. J. (1976). The storage of low grade thermal energy using phase change materials. *Appl. Energy* 2, 205–216. doi: 10.1016/0306-2619(76)90025-8
- Ren, Y. J., and Ruckman, J. E. (2004). Condensation in three-layer waterproof breathable fabrics for clothing. *Int. J. Cloth. Sci. Technol.* 16, 335–347. doi: 10.1108/09556220410527255
- Rigotti, D., Dorigato, A., and Pegoretti, A. (2018). 3D printable thermoplastic polyurethane blends with thermal energy storage/release capabilities. *Mat. Today Commun.* 15, 228–235. doi: 10.1016/j.mtcomm.2018.03.009
- Robaidi, A. A. (2013). Development of novel polymer phase change material for heat storage application. *Int. J. Mat. Sci. Appl.* 2, 168–172. doi: 10.11648/j.ijmsa.20130206.11
- Sari, A., Akcay, M., Soylak, M., and Onal, A. (2005). Polymer-stearic acid blends as form-stable phase change material for thermal energy storage. *J. Sci. Ind. Res.* 64, 991–996.
- Sari, A., and Soylak, M. (2007). Equilibrium and thermodynamic studies of stearic acid adsorption on Celtek clay. *J. Serbian Chem. Soc.* 72, 485–494. doi: 10.2298/JSC0705485S
- Sarier, N., and Onder, E. (2012). Organic phase change materials and their textile applications: An overview. *Thermochim. Acta* 540, 7–60. doi: 10.1016/j.tca.2012.04.013
- Sharma, R. K., Ganesan, P., Tyagi, V. V., Metselaar, H. S. C., and Sandaran, S. C. (2015). Developments in organic solid-liquid phase change materials and their applications in thermal energy storage. *Energy Convers. Manag.* 95, 193–228. doi: 10.1016/j.enconman.2015.01.084
- Shim, H., McCullough, E. A., and Jones, B. W. (2001). Using phase change materials in clothing. *Text. Res. J.* 71, 495–502. doi: 10.1177/004051750107100605
- Shin, Y., Yoo, D.-I., and Son, K. (2005). Development of thermoregulating textile materials with microencapsulated phase change materials (PCM). II. Preparation and application of PCM microcapsules. *J. Appl. Polymer Sci.* 96, 2005–2010. doi: 10.1002/app.21438
- Sobolciak, P., Karkri, M., Al-Maaded, M. A., and Krupa, I. (2016). Thermal characterization of phase change materials based on linear low-density polyethylene, paraffin wax and expanded graphite. *Renew. Energy* 88, 372–382. doi: 10.1016/j.renene.2015.11.056
- Su, J. F., Wang, S. B., Zhang, Y. Y., and Huang, Z. (2010). Physicochemical properties and mechanical characters of methanol-modified melamine-formaldehyde (MMF) shell microPCMs containing paraffin. *Colloid Polym. Sci.* 289, 111–119. doi: 10.1007/s00396-010-2328-1
- Su, J. F., Wang, X. Y., and Dong, H. (2012a). Micromechanical properties of melamine-formaldehyde microcapsules by nanoindentation: effect of size and shell thickness. *Mater. Lett.* 89, 1–4. doi: 10.1016/j.matlet.2012.08.072
- Su, J. F., Wang, X. Y., Wang, S. B., Zhao, Y. H., Zhu, K. Y., and Yuan, X. Y. (2011). Interface stability behaviors of methanol-melamine-formaldehyde shell microPCMs/epoxy matrix composites. *Polymer Compos.* 32, 810–820. doi: 10.1002/pc.21102
- Su, J. F., Zhao, Y. H., Wang, X. Y., Dong, H., and Wang, S. B. (2012b). Effect of interface debonding on the thermal conductivity of microencapsulated-paraffin filled epoxy matrix composites. *Compos. A Appl. Sci. Manuf.* 43, 325–332. doi: 10.1016/j.compositesa.2011.12.003
- Trigui, A., Karkri, M., Boudaya, C., Candau, Y., Ibos, L., and Fois, M. (2014). Experimental investigation of a composite phase change material: thermal-energy storage and release. *J. Compos. Mat.* 48, 49–62. doi: 10.1177/0021998312468185
- Wang, X.-Y., Su, J.-F., Wang, S.-B., and Zhao, Y.-H. (2011). The effect of interface debonding behaviors on the mechanical properties of microPCMs/epoxy composites. *Polymer Compos.* 32, 1439–1450. doi: 10.1002/pc.21174
- Wang, Z. Y., Qiu, F., Yang, W. S., and Zhao, X. D. (2015). Applications of solar water heating system with phase change material. *Renew. Sustain. Energy Rev.* 52, 645–652. doi: 10.1016/j.rser.2015.07.184
- Xi, P., Zhao, F. L., Fu, P., Wang, X. Q., and Cheng, B. W. (2014). Synthesis, characterization, and thermal energy storage properties of a novel thermoplastic polyurethane phase change material. *Mat. Lett.* 121, 15–18. doi: 10.1016/j.matlet.2014.01.128
- Zhang, P., Xiao, X., and Ma, Z. W. (2016). A review of the composite phase change materials: fabrication, characterization, mathematical modeling and application to performance enhancement. *Appl. Energy* 165, 472–510. doi: 10.1016/j.apenergy.2015.12.043

Conflict of Interest Statement: The authors declare that the research was conducted in the absence of any commercial or financial relationships that could be construed as a potential conflict of interest.

Copyright © 2018 Dorigato, Rigotti and Pegoretti. This is an open-access article distributed under the terms of the Creative Commons Attribution License (CC BY). The use, distribution or reproduction in other forums is permitted, provided the original author(s) and the copyright owner(s) are credited and that the original publication in this journal is cited, in accordance with accepted academic practice. No use, distribution or reproduction is permitted which does not comply with these terms.